Received: 20 August 2023 | Revised: 3 March 2024 | Accepted: 18 April 2024

DOI: 10.1002/efd2.153

RESEARCH ARTICLE

eFood WILEY

A study revealing mechanisms behind the stone cell of Yali pear degradation by mixed-culture fermentation of lactic acid bacteria and yeast

Jie Gao[1] | **Chao Xu**[1] | **Guifang Tian**[1] | **Yue Hong Ji**[1] | **Faizan A. Sadiq**[2] | **Ke Wang**[1] | **Yaxin Sang**[1]

[1]College of Food Science and Technology, Hebei Agricultural University, Baoding, China

[2]Advanced Therapies Group, School of Dentistry, Cardiff University, Cardiff, UK

Correspondence

Yaxin Sang, College of Food Science and Technology, Hebei Agricultural University, Baoding 071001, China.
Email: yxsang1418@163.com

Funding information

Hebei Modern Agricultural Industrial Technology System, Grant/Award Number: HBCT2024170206

Abstract

The presence of stone cells in pears is recognized as a problem for the pear processing industry. *Bacillus* and mold can degrade stone cells because of their potential to digest cellulose and lignin, but they cannot be used for the degradation test of pear stone cells. In this study *Lactoplantibacillus plantarum* JYLP-326 was used in single culture or in the mixed culture with *Saccharomyces cerevisiae* Y2 to study their potential to degrade stone cells during fermentation and the mechanism of degradation was further explored. Synergy in cellulase activity was observed in the mixed-culture where the maximum activity was observed at 96th hour of fermentation. Activities of endoglucanase, exoglucanase and β-glucosidase were 1.75, 4.58, and 2.31. The degradation rate of stone cells in the mixed-culture was 37.67%, which was significantly higher than that the results obtained for single cultures. The results of scanning electron microscopy (SEM) showed that the surface of the cultured stone cells became rough. Metabolomics studies confirmed the presence of specific metabolites related to the degradation of stone cells after the fermentation. It was concluded that the mixed-culture fermentation using the above-mentioned strains could be exploited by the pear processing industry to degrade stone cells.

KEYWORDS

cellulose degradation, metabolomics, mixed-culture fermentation, pears, stone cell

1 | INTRODUCTION

At present, the cultivation of pears is limited to Asia, Europe, and America. China is the largest pear producer in the world with an annual production of approximately 18,000,000 tons, which accounts for more than 65% of the world's total production of pears (FAO, 2021). China produces the most diverse varieties of pears that include, but not limited to, *Pyrus bretschneideri Rehd, Pyrus ussuriensis Maxim, (Pyrus pyrifolia [Burm.] Nakai)* and *Pyrus communis Linn*. Pears can be processed into a variety of products, including canned pears, pear wine, pear juice, and pear vinegar and so forth. Pears contain a large amount of dietary fiber (cellulose, hemicellulose, and pectins) that renders juice recovery difficult and any obtained juice is highly turbid and viscous which is difficult to clarify (Zheng et al., 2022). Juice production industries also face similar, but less severe, problems related to turbidity and viscosity in apple juice and orange juice production which is dealt with the use of costly chemical (Sheladiya et al., 2022; Tian et al., 2021). Pear pulp also contains a large number of stone cells or sclereids, which become part of the sediments and affect the quality of the juice especially through their negative

Yaxin Sang contributed equally to this study and should be considered as co-corresponding authors.

effect on mouth feel and sensation. These cells are formed by the secondary deposition of lignin on the primary cell wall of parenchyma cells (Lin et al., 2022). Therefore, apart from the problem of turbidity, proper degradation of stone cells is a prerequisite for the production of fruit juice or wine with good taste.

However, the current research on reducing stone cell content mainly focuses on affecting lignin deposition by changing pollination types (Yan et al., 2023) and genetic manipulation (Xue et al., 2018) through which genes encoding key lignin biosynthesis enzymes are regulated. There are few studies on the degradation of stone cells in pear juice and other processed products. The main components of stone cells are lignin (20%), cellulose (52%), and hemicellulose (23%) (Mamat et al., 2021). Cellulose is an unbranched chain of polymer of glucose monomers linked by β-1,4 glycosidic bonds. Hydrogen bonds can be formed within and between cellulose molecules, and the existence of these structures hinders the degradation of cellulose (Wang, Wang, et al., 2022). Therefore, breaking inter- and intramolecular chemical bonds and reducing the crystallinity of cellulose are key to its degradation. Stone cell degradation also requires lignin degradation which is made up of three phenylpropane units (syringyl, guaiacyl, and p-hydroxyphenyl) that are linked to each other through ether and carbon–carbon bonds (Zhang & Wang, 2020)—making stone cells more resilient against degradation (Wu et al., 2022; Yingjie et al., 2018). Compared with cellulose and lignin, hemicellulose is relatively easy to be degraded. However, hemicellulose is usually intertwined with cellulose and lignin through hydrogen and covalent bonds that makes its degradation difficult without any prior degradation of cellulose and lignin (Chen et al., 2022) (Supporting Information S1: Figure 1). Therefore, the degradation of lignin and cellulose in stone cells is the key challenge.

Literature shows that the current research on cellulose and lignin degradation mainly focuses on straw degradation to improve composting and lignocellulosic biomass processing for the production of new biofuels (Langan et al., 2011). No research has focused on the degradation of the same elements in pear stone cells. Since the composition of stone cells is similar to that of lignocellulose, degradation techniques can be applied on stone cells too. To reduce energy consumption and protect the environment, biological methods are highly demanding (Li, Han, et al., 2020; Zhu et al., 2021). Liu et al. used actinomycetes to degrade cellulose, lignin, and hemicellulose in maize straws (Liu et al., 2022). *Aspergillus sydowii* C6d, isolated from the rumen of camel, is a novel fungal strain with lignocellulosic degradation capacity (Tulsani et al., 2022). It can be concluded that most of these strains are molds, bacilli or actinomycetes, but these microorganisms cannot be used in pear juice to degrade stone cells or for any other functional applications. Findings from previous research show that the use of single strain in lignocellulose degradation is less effective and a combined use of multiple strains shows effective results. For instance, a mixed-culture system of *Serratia sp*. AXJ-M and *Arthrobacter sp*. AXJ-M1 was shown to significantly improve the degradation rate of cellulose in paper black liquor (An et al., 2022), and similarly, the mixed-culture of *Phanerochaete chrysosporium* and *Trichoderma viride* effectively improved the degradation efficiency of straws (Chen et al., 2019). These studies further indicate that when multiple microorganisms are co-cultured and an optimal culture mode is established, it can create a more favorable growth environment for various strains. This enhancement in the growth milieu leads to an upregulation of related enzyme genes within the culture system. Consequently, there is an increase in both enzyme concentration and activity, thereby facilitating more efficient degradation of lignocellulose (Detain, Remond, et al., 2022; Shi et al., 2020)

Currently, lactic acid bacteria and yeast are commonly used in pear processing. Lactic acid bacteria are widely used in healthy and functional food formulations where a repertoire of their metabolites improve the aroma and nutritional profile of the product (Wang, Zhang, et al., 2022; Yang et al., 2022). It is well known that lactic acid bacteria and yeast are often used in mixed-culture systems (e.g., fermentation of cocoa beans, coffee, milk, and sourdough) where they perform better in terms of overall metabolic activities and functional characteristics of interest like aroma and taste (Perez-Alvarado et al., 2022; Viesser et al., 2021; Zhang, Dai, et al., 2021). However, there are few lactic acid bacteria or yeast species that can be used in monoculture for efficient degradation of stone cells in food because they rarely produce enzymes that can degrade stone cells. At present, the literature shows that *Lactoplantibacillus plantarum* has genes related to the expression of cellulase, Zhao et al. improved the quality of alfalfa silage by using *L. plantarum* that can express lignocellulose degradation-related enzyme genes (Zhao et al., 2020). Therefore, given that *L. plantarum* is classified as Generally Regarded As Safe (GRAS), it not only enhances the nutritional value and aroma of pear juice products but also exhibits cellulose-degrading properties. Therefore, we selected *L. plantarum* as the key fermenting culture. An exploration of major strain libraries revealed that strains like *L. plantarum* JYLP-326, CICC 24435, and CICC 24437 are capable of producing cellulases that can break down the cellulose in stone cells, suggesting their potential for stone cell degradation. Furthermore, to enhance this degradation capability, we conducted a study on the acquired *L. plantarum* strains. We co-cultured them with yeast strains, specifically *Saccharomyces cerevisiae Y2 or Kazachstania unispora SXJ*. The purpose was to identify the most efficacious yeast strain for synergistic co-culturing with *L. plantarum*, aimed at optimizing stone cell degradation. By comparing the changes of surface structure, internal functional groups and crystallinity of stone cells, the degradation effect of composite strains on stone cells was described.

Finally, the degradation pathway of stone cells was studied by metabolomics.

2 | MATERIALS AND METHODS

2.1 | Materials

S. cerevisiae Y2 (NCBI accession number KT732655.1) and *K. unispora* SXJ were isolated from Kefir grains (NCBI accession number MK268124.1). *L. plantarum* (CICC 24435) and *L. plantarum* (CICC 24437) were purchased from the China Center of Industrial Culture Collection. *L. plantarum* JYLP-326 were purchased from the Shandong Zhongke-Jiayi Bioengineering Co. Ltd.

2.2 | Strains and culture conditions

Three strains of *L. plantarum* were incubated in MRS (Aoboxing) liquid medium at 37°C. *S. cerevisiae* Y2 and *K. unispora* SXJ were incubated in Yeast Extract Peptone Dextrose (YPD) medium (20 g/L glucose, 20 g/L peptone, 10 g/L yeast extract; w/v) at 28°C (Aoboxing).

L. plantarum JYLP-326 (2×10^7 CFU/mL) was mixed-culture with *S. cerevisiae* (4.2×10^5 CFU/mL) Y2 in stone cell liquid medium (20 g/L stone cells, 10 g/L peptone, 10 g/L beef extract, 5 g/L yeast extract, 2 g/L ammonium citrate, 2 g/L K2HPO4, 5 g/L NaAc, 0.2 g/L MgSO4, 0.05 g/L MnSO4, 1 mL Tween-80; pH 6.7 ± 0.2; w/v) and incubated at 30°C (120 r/min) for 96 h (Renye et al., 2021).

2.3 | Determination of enzyme activity

Three strains of *L. plantarum* were inoculated into MRS broth medium with pH value of 6.3 ± 0.2 at an inoculum of 2×10^7 CFU/mL and incubated for 24 h at 30°C in a shaker at 120 r/min to prepare a preculture medium. Subsequently, *S. cerevisiae* Y2 and *K. unispora* SXJ were inoculated into the preculture medium at an inoculum of 4.2×10^5 CFU/mL. The culture temperature and shaking speed remained unchanged, and the culture time lasted for 96 h. During this period, samples were taken every 24 h, centrifuged at 8000 r/min for 10 min at 4°C, and the supernatant, which is the crude enzyme solution, was taken, and the tests were grouped as shown in Figure 1 (Li, Zhang, et al., 2022).

The enzyme activity of the obtained crude enzyme solution was determined using the dinitrosalicylic acid (DNS) colorimetric method (Li, Xie, et al., 2020). The substrates corresponding to endoglucanase, exoglucanase, β-glucosidase and filter paper enzymes were sodium carboxymethyl cellulose, microcrystalline cellulose, salicin and Whatman No. 1 filter paper, respectively (Dobrzynski et al., 2022). 0.5 mL of crude enzyme solution was dissolved in 1.5 mL of citrate buffer (containing 1% CMC-Na, microcrystalline cellulose, salicin, and 50 mg of filter paper) and incubated for 50 min at 50°C. Then, 2 mL of DNS reagent was added to the citrate buffer. The mixture was boiled for 10 min and then cooled to room temperature. Then the volume was adjusted to 20 mL with distilled water, and then oscillated violently. The absorbance of the mixture at OD_{540} was measured. The amount of glucose in the enzyme solution was determined from the glucose standard curve and thus the enzyme activity was calculated. One unit (U) of enzyme activity was defined as the amount of enzyme that catalyzes the hydrolysis of the substrate solution to produce 1 μM of glucose per minute (Balla et al., 2022).

2.4 | Determination of cellulose content in stone cells in nine groups of fermentation broth before and after fermentation

Three strains of *L. plantarum* and two strains of yeast were inoculated into the stone cell liquid fermentation medium according to 2.2 and incubated in a shaker at 30°C at 120 r/min. Samples were taken after 96 h of fermentation, and the stone cells were dried in an oven at 50°C to a constant weight. Subsequently, the cellulose content of the stone cells in the nine groups of samples was determined using a cellulose content assay kit (Solarbio) The changes in the cellulose content of the stone cells in the nine groups of samples were determined using a Solarbio kit.

2.5 | Determination of the degradation rate of stone cells after individual and mixed-culture

The degradation rate of stone cells was determined using the weight method (Qinggeer et al., 2016), The degradation rate of stone cells fermented by *L. plantarum* JYLP-326 alone and mixed-culture fermentation by *L. plantarum* JYLP-326 and *S. cerevisiae* Y2 for 96 h was determined by weight method. The sample preparation method is the same as 2.3, and the degradation rate of stone cells was calculated as follows.

$$\text{Degradation rate}(\%) = \frac{m1 - m2}{m1} \times 100,$$

$m1$ represents the amount of stone cells in the medium before fermentation, and $m2$ represents the amount of stone cells in the medium after fermentation.

2.6 | Changes in the apparent structure of stone cells before and after fermentation

Referring to the method of Imran (Pasha et al., 2021) with slight modifications: The Czech TESCAN MIRA

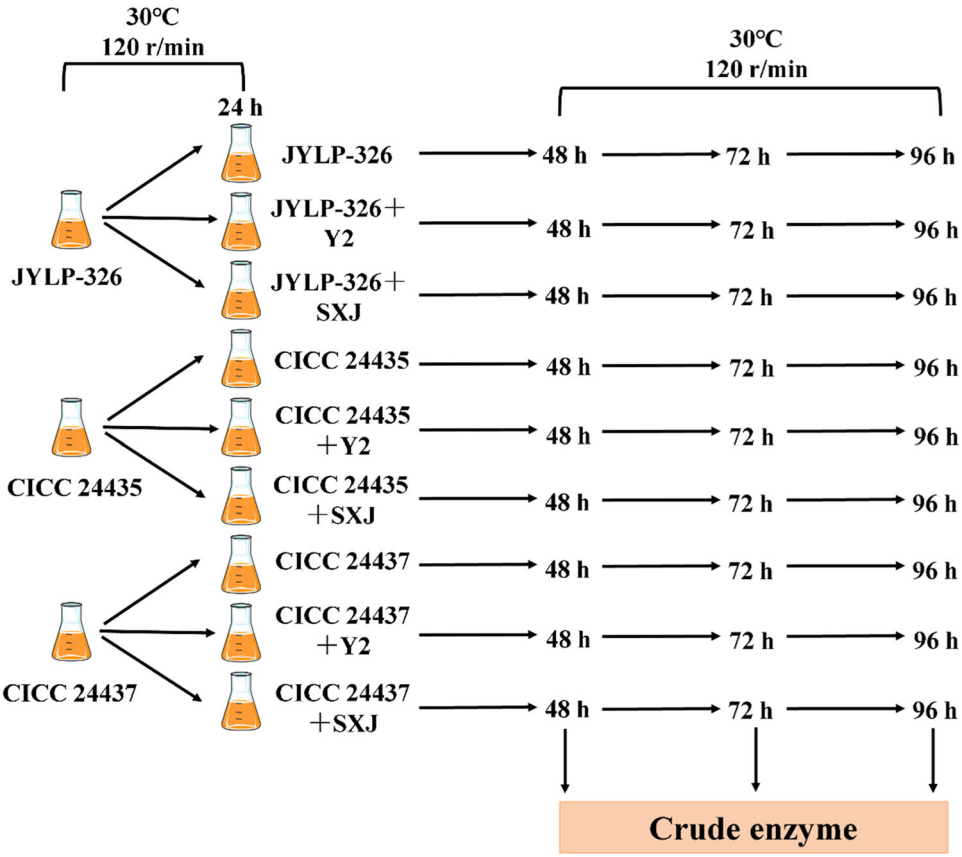

FIGURE 1 Grouping of cellulose enzyme activity assays. CICC 24435, *Lactoplantibacillus plantarum* CICC 24435; CICC 24435+SXJ, *Lactoplantibacillus plantarum* CICC 24435 and *Kazachstania unispora* SXJ; CICC 24435+Y2, *Lactoplantibacillus plantarum* CICC 24435 and *Saccharomyces cerevisiae* Y2; CICC 24437, *Lactoplantibacillus plantarum* CICC 24437; CICC 24437+SXJ, *Lactoplantibacillus plantarum* CICC 24437 and *Kazachstania unispora* SXJ; CICC 24437+Y2, *Lactoplantibacillus plantarum* CICC 24437 and *Saccharomyces cerevisiae* Y2; JYLP-326, *Lactoplantibacillus plantarum* JYLP-326; JYLP-326+SXJ, *Lactoplantibacillus plantarum* JYLP-326 and *Kazachstania unispora* SXJ; JYLP-326+Y2, *Lactoplantibacillus plantarum* JYLP-326 and *Saccharomyces cerevisiae* Y2. The culture condition was 30°C 120 r/min and the sampling time was 48, 72, 96 h.

LMS scanning electron microscope (SEM) was used to observe the untreated and treated stone cells. Appropriate amount of stone cells were taken, placed on conductive tape, and sprayed with gold for 45 s using an Oxford Quorum SC7620 sputter coating instrument. The sample stage was placed into the scanning electron microscope, evacuated and observed. The acceleration voltage was 3 KV and the image scanning multiple was ×500, ×2000, and ×5000.

2.7 | Changes in the chemical structure of stone cells before and after fermentation

A Thermo Scientific Nicolet iS20 Fourier transform infrared spectrometer (FTIR) was used for infrared scanning of the samples. A small amount of untreated and treated stone cells after constant weight were taken respectively, and an appropriate amount of KBr was added, and the samples were ground evenly in an agate mortar and pressed to process. During the test, the background (KBr) was collected first, and then the infrared spectrum of the sample was collected. The resolution was 4 cm^{-1}, the number of scans was 32, and the test won-number range was 400–4000 cm^{-1} (Danso et al., 2022).

2.8 | Changes in crystallinity of stone cells before and after fermentation

According to the method of Ma (Ma et al., 2022) with slight modifications: untreated and treated stone cell samples were detected using an X-ray diffractometer (XRD) (Rigaku SmartL ab SE). The specific conditions were as follows: Cu target, tube pressure of 40 KV, current of 40 mA, scanning rate of 2°/min, and scanning range of 5–80°. The crystallinity index was calculated as follows (Kim et al., 2018):

$$\mathrm{CrI} = \frac{I_{002} - \mathrm{Iam}}{I_{002}} \times 100.$$

I_{002} represents the crystalline area of the cellulose component in the biomass diffraction peak intensity, $2\theta \approx 22°$, and Iam represents the amorphous area of the cellulose component in the biomass diffraction peak intensity, $2\theta \approx 18°$.

2.9 | Untargeted metabolomics analysis of stone cells before and after mixed-culture fermentation

The stone cell culture medium of *L. plantarum* JYLP-326 and *S. cerevisiae* Y2 mixed-cultured for 0 and 96 h was divided into supernatant and stone cells. The stone cells were dried by drying under the same conditions as 2.2 and the supernatant was freeze-dried by vacuum. Then, metabolomics detection was performed according to the method of Shi et al. (Zhou et al., 2020). The data were analyzed on the online platform of Majorbio Cloud Platform (www.majorbio.com).

2.10 | Statistical analysis

All the experiments were conducted in triplicate. All data were reported as mean ± standard error of the mean ($n = 3$). One-way ANOVA was applied to compare multiple treatments with Duncan's test by using IBM SPSS Statistics 25.0 at the significance level of $p < 0.05$. The graphs were plotted using Origin 2022.

3 | RESULTS

3.1 | Cellulase production under single and mixed-culture conditions

The results of clear zone test on CMC medium with iodine and the filter paper degradation test showed that all three strains of *L. plantarum* had the potential to degrade cellulose (Supporting Information S1: Figure 2).

Filter paper (Fpase), endoglucanase (CMCase), exoglucanase (PNPCase), and β-glucosidase (PNPGase) activity assays were performed to determine the capacity of *L. plantarum* strains to produce cellulase in single culture or in different dual-species cultures in which they were grown with *S. cerevisiae* Y2 and *K. unispora* SXJ (Table 1).

Overall, LPY.1 produced 4.58 U/mL of exoglucanase, which was the highest among all cellulase enzymes, and filter paper enzyme activity (2.04 U/mL) was the lowest. Cellulase activity of all groups did not increase after 96 h of fermentation, and for endoglucanase we observed that LP.1 (96 h), LPY.1 (72 and 96 h), LPS.2 (48, 72, and 96 h), LPS.3 (48 h), and LPY.3 (48 and 72 h) groups showed higher enzyme activity compared to the other groups, which were not significantly different. Therefore, the best composite strain could not be screened by endoglucanase.

It was noticed that exoglucanase/cellobiohydrolase showed the highest activity in all enzyme activity determination experiments (Table 1). Compared with single cultures of *L. plantarum* strains, the exoglucanase activity of dual-species cultures was higher. (Table 1). When LPY.1 was mixed-cultured for 96 h, the enzyme activity reached to the maximum level of 4.58 U/mL, and the enzyme activity of this group was significantly higher than other groups. Moreover, except for the two groups that contained both *L. plantarum* and the yeast (LPY.1 and LPS.2), enzymatic activities decreased after 72 h of culturing and the highest value of the enzyme was recorded as 2.99 U/mL, which was produced by the LPY.2 group at 72 h of culture.

In terms of β-glucosidase, all groups showed an increase in enzyme activity during incubation, except for one group in which *L. plantarum* JYLP-326 was cultured alone. The maximum value of enzyme activity (2.40 U/mL) after 72 h of incubation was observed in group LPY.1. This value was not significantly different from the enzymatic activity values noted for groups LPY.1 (96 h) and LPS.3 (72 h) (Table 1).

In all enzyme activity determination experiments, filter paper enzyme activity was low. Except LP.3 group, the filter paper enzyme activity of other groups increased with the prolongation of culture time. The highest filter paper enzyme activity was observed for LPY.1 group. When LPY.1was mixed-cultured for 96 h, the enzyme activity reached 2.04 U/mL, which was significantly higher than the enzyme activities recorded for other groups. Cellulose degradation is the result of the synergistic action of cellulases (Yang et al., 2021). LPY.1 group showed the best performance in all enzyme activities and was initially selected as the optimal group of mixed strains (Table 1).

3.2 | Changes in cellulose content in stone cells under individual and mixed-culture conditions

From our trials on measuring the cellulase activity of single and mixed cultures, 96 h was identified as the optimum time for fermentation, therefore, samples at 0 and 96 h of fermentation were selected for the next study. We measured leftover cellulose content in stone cells at 96 h of fermentation that was carried out by the above mentioned nine groups of single and mixed cultures. The test results are shown in Figure 2A. Cellulose content of stone cells reduced significantly after 96 h of fermentation with different groups. Lowest cellulose content (57.98 mg/g), as a result of 82.26% cellulose degradation, was observed when stone cells underwent fermentation with group JYLP-326 + Y2. Therefore, JYLP-326 + Y2

TABLE 1 Variation of cellulase activity with fermentation time under single and mixed-culture.

	Fermentation time/h	LP.1	LPS.1	LPY.1	LP.2	LPS.2	LPY.2	LP.3	LPS.3	LPY.3
CMCase (U/mL)	48	1.21 ± 0.22^{cdeB}	1.31 ± 0.14^{bcdA}	1.57 ± 0.19^{bcB}	0.82 ± 0.17^{eB}	1.75 ± 0.26^{ab}	1.31 ± 0.46^{bcd}	0.96 ± 0.11^{de}	1.65 ± 0.20^{abc}	2.04 ± 0.27^{a}
	72	1.20 ± 0.11^{cdB}	1.55 ± 0.24^{abcA}	2.08 ± 0.36^{aA}	0.95 ± 0.08^{dB}	1.95 ± 0.72^{ab}	1.51 ± 0.06^{bc}	1.48 ± 0.17^{bcd}	1.44 ± 0.05^{bcd}	1.76 ± 0.09^{ab}
	96	2.03 ± 0.03^{aA}	1.68 ± 0.49^{abcA}	1.75 ± 0.02^{abAB}	1.27 ± 0.23^{cdeA}	1.85 ± 0.27^{ab}	1.12 ± 0.16^{e}	$1.57 \pm 0.23b^{cd}$	0.65 ± 0.14^{f}	1.19 ± 0.08^{de}
	120	0.81 ± 0.16^{bC}	–	–	1.25 ± 0.05^{aA}	–	–	–	–	–
PNPCase (U/mL)	48	$1.28 \pm 0.23^{\mathbf{eB}}$	$2.81 \pm 0.19^{\mathbf{bA}}$	4.09 ± 0.47^{aA}	1.75 ± 0.16^{dA}	2.49 ± 0.03^{bcB}	2.31 ± 0.21^{cB}	1.39 ± 0.20^{deC}	1.04 ± 0.16^{eC}	1.75 ± 0.05^{dB}
	72	$1.92 \pm 0.08^{\mathbf{eA}}$	$2.94 \pm 0.28^{\mathbf{bA}}$	4.07 ± 0.42^{aA}	1.12 ± 0.30^{f}	2.01 ± 0.22^{deC}	2.99 ± 0.10^{bA}	2.73 ± 0.26^{bcA}	2.89 ± 0.13^{bA}	2.37 ± 0.14^{cdA}
	96	$1.18 \pm 0.07^{\mathbf{eB}}$	$2.02 \pm 0.28^{\mathbf{cdB}}$	4.58 ± 0.78^{aA}	$1.47 \pm 0.27d^{eAB}$	3.02 ± 0.10^{bA}	2.14 ± 0.19^{cB}	2.09 ± 0.26^{cB}	1.88 ± 0.14^{cdB}	1.63 ± 0.25^{cdeB}
	120	–	–	3.65 ± 0.28^{aA}	1.41 ± 0.29^{cAB}	2.08 ± 0.19^{bC}	–	–	–	–
PNPGase (U/mL)	48	1.78 ± 0.06^{abA}	1.47 ± 0.15^{bcB}	1.66 ± 0.05^{abB}	1.18 ± 0.13^{cA}	1.47 ± 0.20^{bcB}	1.56 ± 0.35^{bcAB}	1.17 ± 0.12^{cB}	2.02 ± 0.43^{aA}	1.46 ± 0.12^{bcA}
	72	1.58 ± 0.04^{dA}	1.82 ± 0.31^{cdAB}	2.40 ± 0.17^{aA}	1.06 ± 0.10^{eA}	1.98 ± 0.10^{bcA}	1.84 ± 0.11^{cdA}	1.58 ± 0.13^{dA}	2.17 ± 0.10^{abA}	1.72 ± 0.23^{cdA}
	96	1.58 ± 0.21^{cdA}	1.91 ± 0.03^{bA}	2.31 ± 0.12^{aA}	1.21 ± 0.14^{eA}	1.19 ± 0.08^{eC}	1.24 ± 0.14^{eB}	1.74 ± 0.17^{bcA}	1.63 ± 0.17^{cdA}	1.46 ± 0.17^{deA}
	120	–	–	–	–	–	–	–	–	–
Fpase (U/mL)	48	0.59 ± 0.03^{dC}	1.04 ± 0.19^{abA}	0.75 ± 0.08^{cdB}	0.73 ± 0.21^{dB}	1.24 ± 0.08^{aB}	0.78 ± 0.15^{bcdC}	1.14 ± 0.02^{aA}	1.00 ± 0.24^{abcAB}	1.08 ± 0.08^{aB}
	72	0.67 ± 0.02^{cdBC}	1.00 ± 0.03^{abA}	1.11 ± 0.11^{aB}	0.74 ± 0.20^{bcdB}	1.11 ± 0.07^{aB}	1.06 ± 0.12^{aBC}	0.63 ± 0.16^{dC}	0.91 ± 0.33^{abcdB}	0.95 ± 0.06^{abcB}
	96	1.46 ± 0.05^{bcA}	1.19 ± 0.11^{dA}	2.04 ± 0.32^{aA}	1.71 ± 0.10^{bA}	1.39 ± 0.05^{cdA}	1.45 ± 0.08^{cA}	0.85 ± 0.02^{eB}	1.49 ± 0.15^{bcA}	1.49 ± 0.13^{bcA}
	120	0.80 ± 0.14^{cB}	–	1.01 ± 0.10^{bcB}	1.54 ± 0.14^{aA}	1.11 ± 0.09^{bB}	1.27 ± 0.23^{abAB}	–	–	–

Note: All the data are expressed as mean ± SD. Different letters indicate at $p < 0.05$ significant difference in different groups, mention the differences between cultures in a specific time with small letters and show the differences between times in a specific culture with capital letters.

Abbreviations: CMCase, endoglucanase; Fpase, filter paper enzyme; LP.1, *Lactoplantibacillus plantarum* JYLP-326; LP.2, *Lactoplantibacillus plantarum* CICC 24435; LP.3, *Lactoplantibacillus plantarum* CICC 24437; LPS.1, *Lactoplantibacillusplantarum* JYLP-326 and *Kazachstania unispora* SXJ; LPS.2, *Lactoplantibacillus plantarum* CICC 24435 and *Kazachstania unispora* SXJ; LPS.3, *Lactoplantibacillus plantarum* CICC 24437 and *Kazachstania unispora* SXJ; LPY.1, *Lactoplantibacillus plantarum* JYLP-326 and *Saccharomyces cerevisiae* Y2; LPY.2, *Lactoplantibacillus plantarum* CICC 24435 and *Saccharomyces cerevisiae* Y2; LPY.3, *Lactoplantibacillus plantarum* CICC 24437 and *Saccharomyces cerevisiae* Y2; PNPCase, exoglucanase; PNPGase, β glucosidase; -, cellulase activity of specific cultures was no longer increased or decreased after 96 h of fermentation.

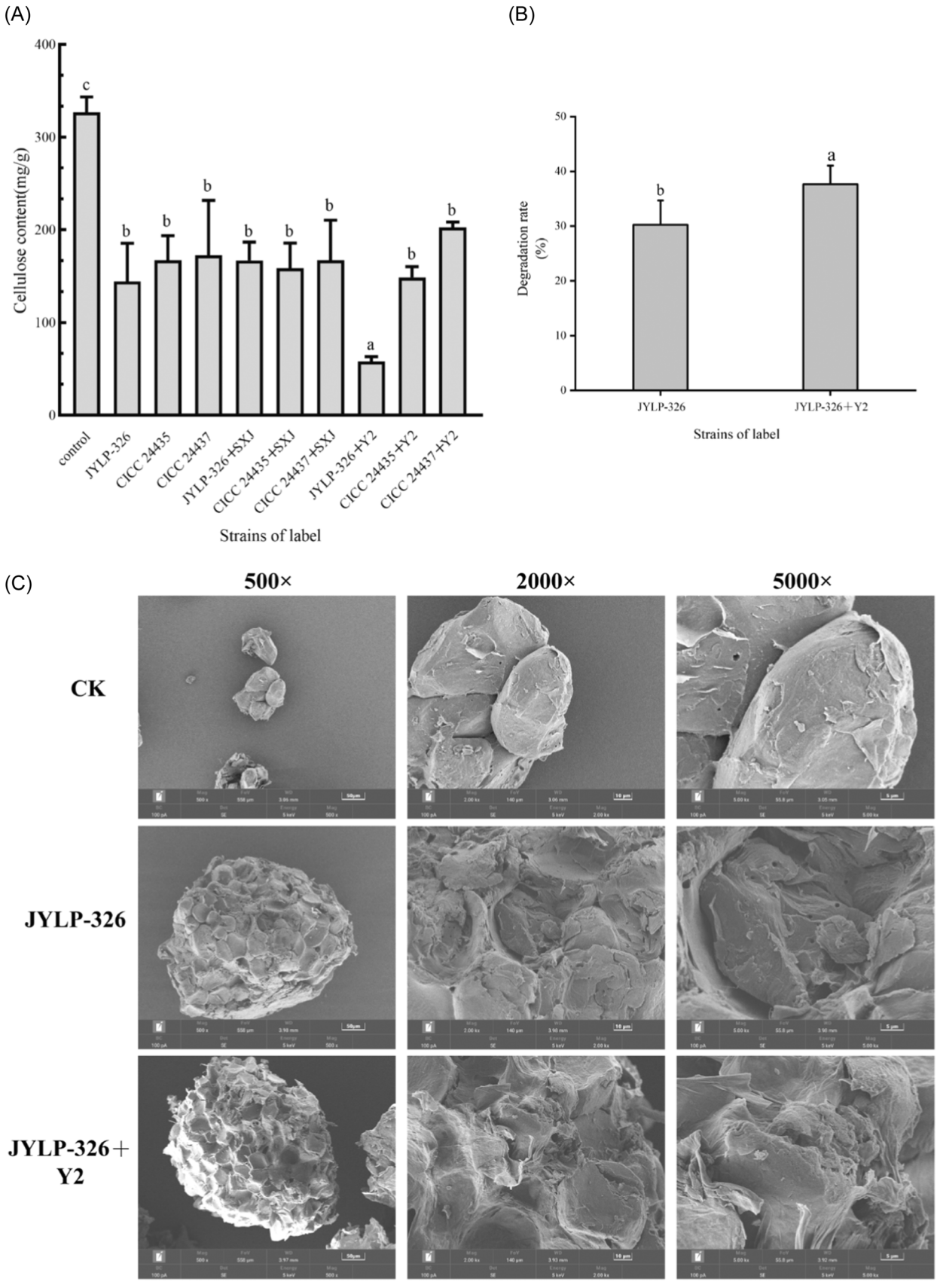

FIGURE 2 (See caption on next page).

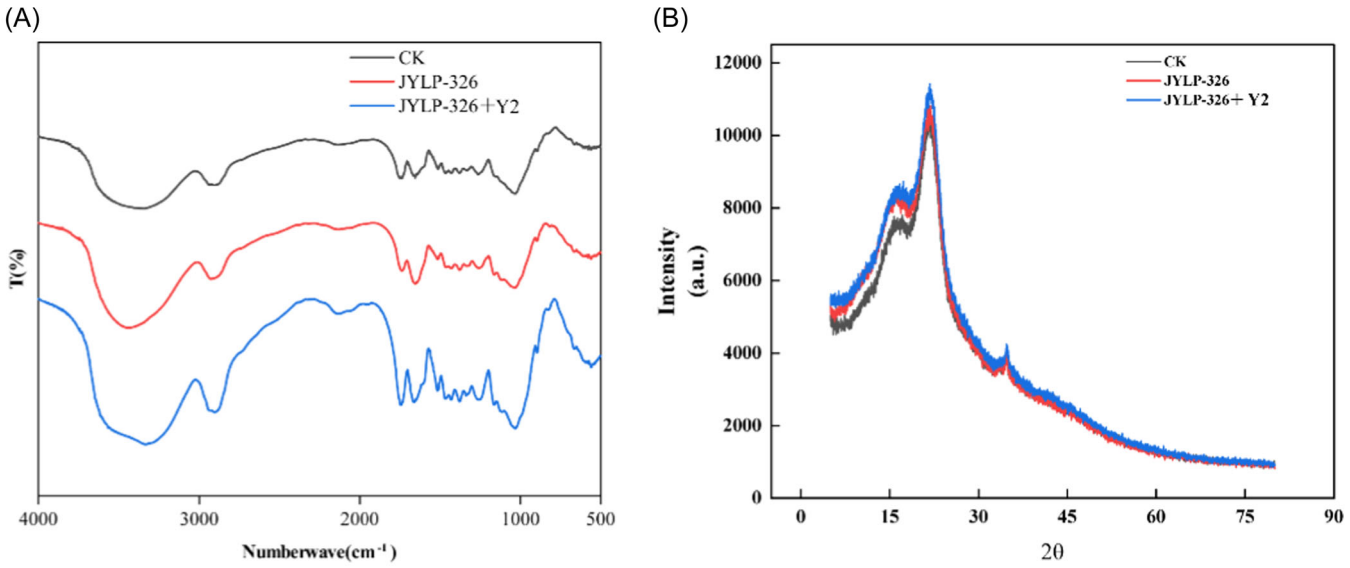

FIGURE 3 FTIR (A) and X-ray diffractometer (B) patterns of single and mixed-culture.

was the best strain combination for degrading stone cells and the following study was conducted using JYLP-326 + Y2 group.

3.3 | Changes in the degradation rate of stone cells and apparent structure of stone cells under single and mixed-culture conditions

This part of the work was carried out with three groups, namely CK (an unfermented blank control group), JYLP-326 (fermentation with *L. plantarum* JYLP-326) and JYLP-326 + Y2 (fermentation with mixed cultures comprising *L. plantarum* JYLP-326 and *S. cerevisiae* Y2). Compared with the degradation rate of stone cells fermented by single strain *of L. plantarum* alone (30.25%), the degradation rate of stone cells fermented by mixed-culture fermentation reached 37.67%, which was significantly higher than that of single fermentation group (Figure 2B). Apparent structural changes in stone cells following fermentation under the above-mentioned conditions were observed by scanning electron microscopy (SEM) (Figure 2C). Observations revealed that the untreated stone cells, categorized in the CK group CK, exhibited a flat, smooth surface with a tight, intact structure, rendering the internal structure of these cells barely discernible. In contrast, stone cells treated with *L. plantarum* JYLP-326 demonstrated a distinctly uneven surface characterized by a slightly rough, honeycomb-like texture, marked by the presence of small holes and fissures. Furthermore, stone cells subjected to fermentation with the mixed-culture displayed a notably more rugged and frayed appearance. This treatment resulted in a surface that became markedly rugged, with a more visible internal structure. The observed alterations included an increase in pore size and an enlargement of the existing cracks. This indicates that the structure of the stone cells was damaged after fermentation and it was highest in case of mixed-culture fermentation.

3.4 | Changes in the chemical structure of stone cells under single and mixed-culture fermentation

Figure 3A and Supporting Information S1: Table 1 show the FTIR spectra and characteristic peaks of stone cells subjected to single and mixed-culture fermentation. The characteristic peaks of cellulose, lignin, and hemicellulose in stone cells are mainly shown in Figure 3A. The characteristic peaks of cellulose appeared at 1031, 1378, 1430, 2902, and 3335 cm^{-1} (Supporting Information S1: Table 1). The characteristic absorption peaks of lignin appeared around 1515 and 1742 cm^{-1}. The absorption

FIGURE 2 Cellulose content (A), stone cell degradation rate (B), and SEM (C) results in single and mixed-culture. CICC 24435, *Lactoplantibacillus plantarum* CICC 24435; CICC 24435 + SXJ, *Lactoplantibacillus plantarum* CICC 24435 and *Kazachstania unispora* SXJ; CICC 24435 + Y2, *Lactoplantibacillus plantarum* CICC 24435 and *Saccharomyces cerevisiae* Y2; CICC 24437, *Lactoplantibacillus plantarum* CICC 24437; CICC 24437 + SXJ, *Lactoplantibacillus plantarum* CICC 24437 and *Kazachstania unispora* SXJ; CICC 24437 + Y2, *Lactoplantibacillus plantarum* CICC 24437 and *Saccharomyces cerevisiae* Y2; JYLP-326, *Lactoplantibacillus plantarum* JYLP-326; JYLP-326 + SXJ, *Lactoplantibacillus plantarum* JYLP-326 and *Kazachstania unispora* SXJ; JYLP-326 + Y2, *Lactoplantibacillus plantarum* JYLP-326 and *Saccharomyces cerevisiae* Y2. Different letters indicate at $p < .05$ significant difference in different groups. *Significant difference between single and mixed-culture ($p < .05$).

peaks near 1258, 1378, and 3335 cm^{-1} represent hemicellulose. The characteristic peaks of lignin appeared around 1515 and 1742 cm^{-1}. The intensity of the absorption peaks of the cells cultured for 96 h by the mixed-culture decreased for nearly all the above wave numbers. While the intensity of the absorption peak of the cells cultured for 96 h by *L. plantarum* JYLP-326 decreased only near 3335 cm^{-1}. This outcome signifies that the primary constituents of stone cells, following microbial mixed-culture fermentation, were efficiently decomposed. This process consequently loosens the surface structure of the stone cells to a notable degree, thereby enlarging the contact area between the stone cells and the microorganisms, facilitating easier degradation. The effective break down of stone cells can substantially reduce the presence of precipitated substances in pome processing products. This improvement in product quality not only enhances the visual appeal for consumers but also promotes the production of pome processing products, contributing to a reduction in resource waste.

3.5 | Changes in crystallinity of stone cells under single and mixed-culture fermentation

The alterations observed in the crystal type and crystallinity of the stone cells reflect the corresponding modifications in the amorphous and crystalline regions of the cellulose within these cells. This phenomenon is indicative of the associated changes in the structural composition of the stone cells. Figure 3B shows the XRD patterns of stone cells. It can be seen that the characteristic diffraction peaks of stone cells from all three groups appear around $2\theta = 16°$, 22°, and 35°, corresponding to the (110), (020), and (004) crystalline planes of I-type cellulose, respectively (Tatsumi et al., 2022), indicating that the crystal type of stone cells did not change after fermentation. However, by comparing the changes in crystallinity, it was found that the crystallinity of stone cells was 29.16% at 0 h of fermentation that showed a decreasing trend until the 96th hour of fermentation. For example, the crystallinity of stone cells decreased from 29.16% to 23.66% and 26.48% in case of single-culture and mixed-culture fermentations, respectively. The decrease in crystallinity means that the cellulose loses its hard hydrogen bond network, making it easier for amorphous cellulose to degrade.

3.6 | Metabolomic profile of stone cells before and after mixed-culture fermentation

3.6.1 | PCA analysis of metabolites in stone cell culture medium before and after fermentation

Overall, 9763 characteristic peaks were extracted from LC-MS/MS total ion chromatogram in the positive ion mode, and a total of 1635 metabolites were identified; 7506 characteristic peaks were extracted in the negative ion mode, and a total of 1564 metabolites were identified. PCA analysis of all identified metabolites showed that the QC samples were clustered into one family in positive and negative ion modes with good instrument stability (Figure 4A,B).

3.6.2 | Differential metabolite analysis before and after fermentation of stone cell medium

OPLS-DA analysis was performed for differential metabolite profiles of supernatant and stone cells before (0 h) and at the 96th hour of fermentation (Figure 4). All groups showed good separation in positive and negative ion modes, indicating significant differences between the groups. OPLS-DA model in the positive ion mode for the supernatant group had the following values: $R^2X = 0.686$, $R^2Y = 0.997$ and $Q^2 = 0.983$ based on the substitution test (Figure 4C,E) In the negative ion mode OPLS-DA model for the supernatant group had the following values: $R^2X = 0.699$, $R^2Y = 0.998$ and $Q^2 = 0.986$ (Figure 4D,F). Similarly corresponding values of R^2X, R^2Y, and Q^2 for stone cells group in positive (Figure 4G,I) and negative (Figure 4H,J) ion modes were 0.446, 0.984, 0.901, and 0.483, 0.98, and 0.906, respectively, indicating that the model has good stability and reliable data.

$p < 0.05$ and VIP > 1.5 were used as screening conditions. Specific differential analysis was performed at 0 and the 96th hour of fermentation for supernatant and stone cell groups (Figure 5). The results indicated a total of 536 differential metabolites for the supernatant group, of which 166 metabolites were upregulated and 370 metabolites were downregulated (Figure 5A). For the stone cell group, 362 differential metabolites were identified, including 175 upregulated metabolites and 187 downregulated metabolites (Figure 5B).

When the above differential metabolites were annotated with the KEGG functional pathways, 94 differential metabolites in the stone cell group were annotated to a wider metabolic category (Figure 5C,D). In the supernatant group, 112 differential metabolites were annotated to a wider range of metabolism. Microbial degradation of lignocellulose mainly involves amino acid metabolism, carbohydrate metabolism, xenobiotics biodegradation and metabolism, metabolism of cofactors and vitamins, and chemical structure transformation maps, so we looked at the differential metabolites that were related to these functional pathways. We found 40 and 36 metabolites in stone and supernatant groups, respectively, that were part of these functional pathways (Table 2).

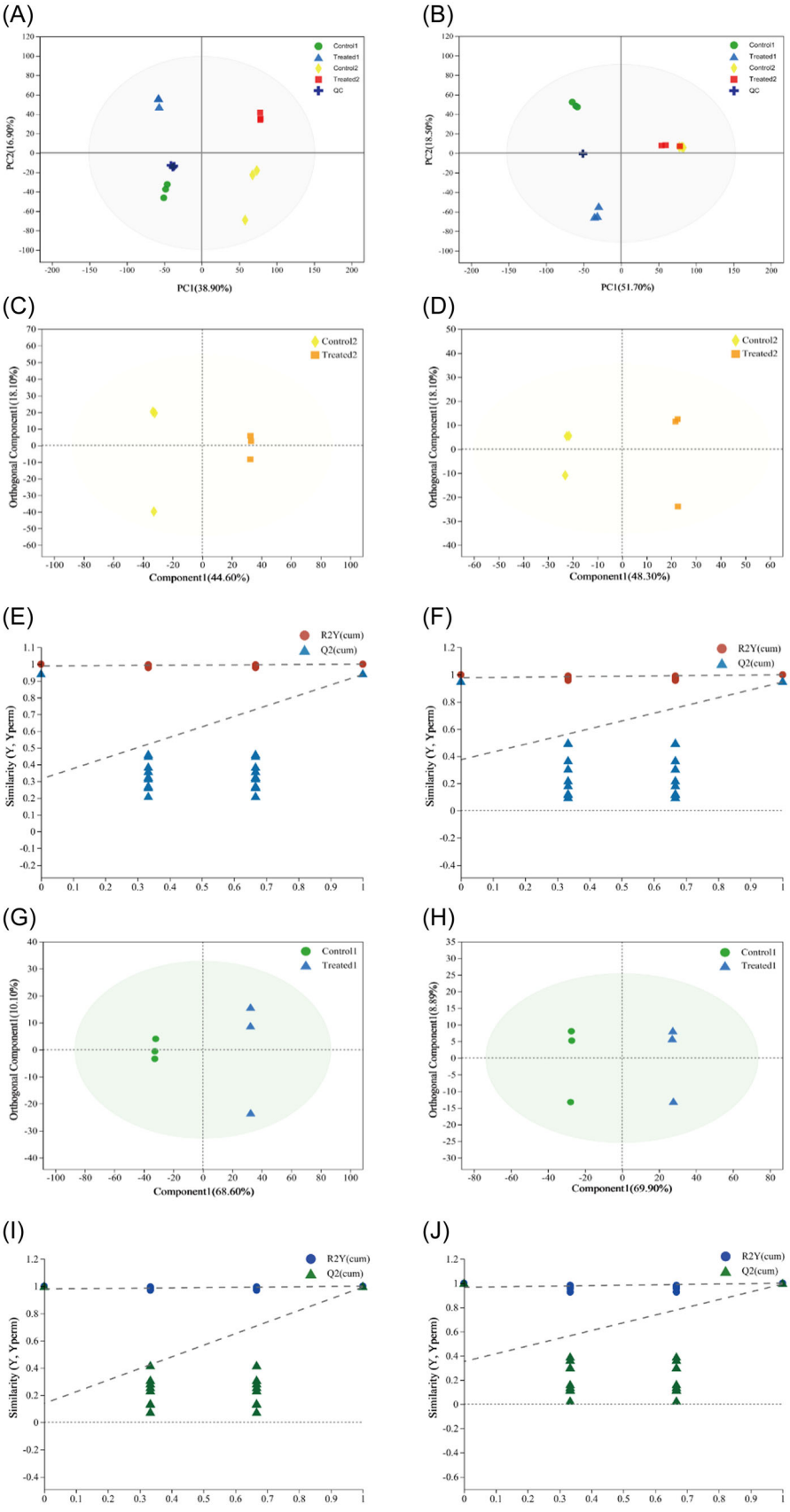

FIGURE 4 (See caption on next page).

3.6.3 | Prediction of metabolic pathways during stone cell degradation

A secondary classification of the differential metabolites into functional pathways was performed (Table 2), which included the following metabolic pathways: galactose metabolism, TCA cycle, fructose and mannose metabolism, starch and sucrose metabolism, amino sugar and nucleotide sugar metabolism, pentose phosphate pathway, pentose and glucuronate interconversions and glyoxylate and dicarboxylic acid metabolism in carbohydrate metabolism; lysine biosynthesis, lysine degradation, arginine biosynthesis, tryptophan metabolism, histidine metabolism, and glycine, serine and threonine metabolism; pantothenate and CoA biosynthesis in metabolism of cofactors and vitamins; biosynthesis of alkaloids derived from shikimate pathway and phenylpropanoid biosynthesis in chemical structure transformation maps.

The metabolic processes involved in some of the metabolites shown in Table 2 were analyzed specifically, and the results are shown in Figure 6. In the stone cell group, the stone cell fermented for 96 h showed an upregulation trend in the relative abundance of differential metabolites related to amino acid metabolic pathway such as tryptophan, 3-Indoleacetic acid, N-hydroxyltryptamine, aspartic acid, L-histidine, imidazole lactic acid, compared to the stone cell fermented at 0 h. N6-acetyl-L-lysine and L-aspartate-semialdehyde. The metabolic pathways annotated by these substances can produce oenzyme A, pyruvate, fumaric acid, and oxoglutaric acid, which are important metabolites in the TCA cycle.

By observing the metabolic processes before and after the fermentation, it was found that malic acid could be produced not only through glycolysis and the TCA cycle, but also through glycolaldehyde via glyoxylate and dicarboxylic acid metabolism. After 96 h of fermentation, level of glycolaldehyde appeared to decrease and stone cells showed abundance of malic acid. A decrease in the abundance of oxoglutaric acid was not surprising since it is produced during various metabolic reactions involving lysine degradation, histidine metabolism, arginine biosynthesis, pentose and glucuronate interconversions and glyoxylate and dicarboxylate metabolism and depleted in lysine biosynthesis, butyrate metabolism, and the TCA cycle.

In addition, several metabolites related to sucrose, galactose, fructose, and mannose metabolism and those produced during the interconversion of pentose and glucuronide (e.g., sucrose, alginose, galactinol, D-mannose 6-phosphate and D-arabinitol) increased in abundance. A decrease in D-galactose abundance in stone cells after 96 h of fermentation was observed.

Compared with the supernatant group at 0 h, the abundance of L-tryptophan, 3-indoleacetic acid, imidazole lactic acid, and L-aspartate-semialdehyde increased at the 96th hour of fermentation, while the abundance of N-hydroxyl-tryptamine, L-histidine, N6-acetyl-L-lysine, aspartic acid, and 5-acetamidovalerate decreased. This indicated that metabolism of the mixed-culture (*L. plantarum* JYLP-326 and *S. cerevisiae* Y2) in supernatant groups and stone cell groups was different. Malic acid and oxoglutaric acid were not found in the supernatant during the screening of differential metabolites. Compared with the supernatant at 0 h, sucrose, D-galactose, trehalose and galactinol contents decreased. It is speculated that some sugars attached to the extracted stone cells were dissolved in the supernatant, and these substances were used as carbon sources to maintain the growth of the mixed-culture (*L. plantarum* JYLP-326 and *S. cerevisiae* Y2) during the fermentation process. An increase in D-mannose 6-phosphate and D-arabinitol contents was presumably related to the degradation of hemicellulose into monosaccharides dissolved in the supernatant.

4 | DISCUSSION

Stone cells are mainly composed of cellulose, lignin, and hemicellulose. Cellulose is the most challenging compound in the degradation of stone cells. Cellulases produced by certain microorganisms can play a key role in the degradation of cellulose present in stone cells (Ajeje et al., 2021; Ren et al., 2019). These cellulases include exoglucanase, endoglucanase, and β-glucosidase (Talebi et al., 2022). Studies have shown that clear zone test on CMC medium with iodine and the filter paper degradation test are the most common methods to test the production of cellulase by microbial strains (Kurnia Ila & Astuti Feb, 2021). The test results showed that the strains used in our experiment had the potential to degrade cellulose, indicating that the tested strains could degrade cellulose.

FIGURE 4 PCA score plot and OPLS-DA score plot of supernatant and stone cell group before and after fermentation. (A and B) show PCA diagram in positive ion and negative modes, respectively. (C and E) show OPLS-DA diagram and permutation test diagram of the supernatant of 0 h versus 96 h fermentation in positive ion mode, respectively. (D and F) show OPLS-DA diagram and permutation test diagram of the supernatant of 0 h versus 96 h fermentation in negative ion mode, respectively. (G and I) show OPLS-DA diagram and permutation test diagram of the stone cells of 0 h versus 96 h fermentation in positive ion mode, respectively. (H and J) show OPLS-DA diagram and permutation test diagram of the stone cells of 0 h versus 96 h fermentation in negative ion mode, respectively. Control1 was the supernatant of 0 h fermentation, Treated1 was the supernatant of 96 h fermentation, Control2 was the stone cells of 0 h fermentation, and Treated2 was the stone cells of 96 h fermentation.

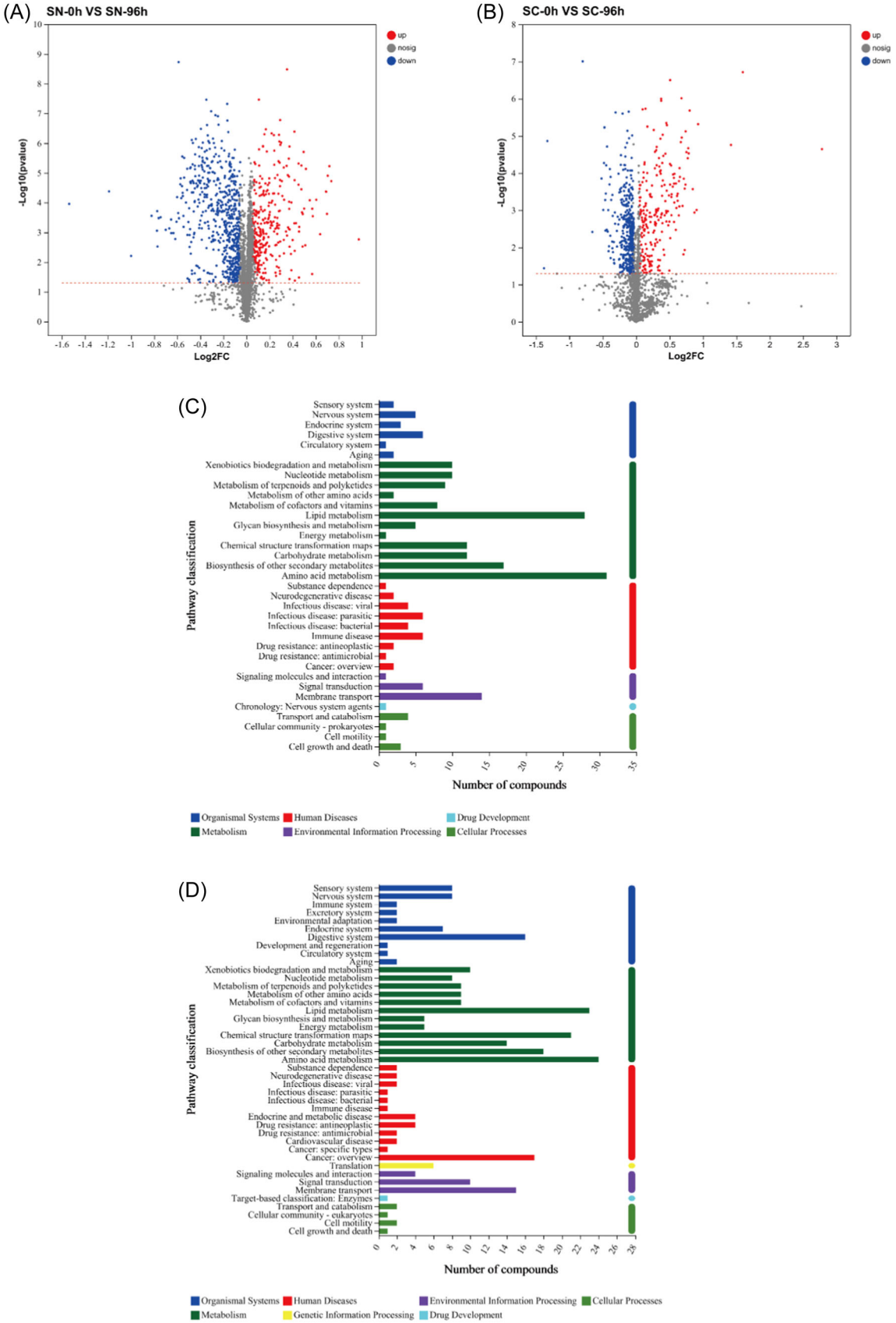

FIGURE 5 Volcano plots of differential metabolites (A and B) and KEGG functional pathway statistics (C and D) (A and C) supernatant; (B and D) stone cells. The differential metabolites were obtained by comparing the fermentation 0 and 96 h, and the metabolic pathway statistics were performed on the screened differential metabolites.

TABLE 2 Differential metabolites in supernatant group and stone cell group.

	VIP	Metabolite	SCZ	SZZ	M/Z
1	2.1929	Malic acid	Up	–	133.0134
2	3.0147	5′-methylthioadenosine	Up	Down	298.0966
3	2.5308	Mevalonic acid	–	Up	190.1072
4	1.7697	D-malic acid	Up	Down	133.0134
5	2.9009	N6-acetyl-L-lysine	–	Down	152.0566
6	2.1951	D-galactose	–	Down	198.0972
7	1.6504	Allysine	Up	Down	332.1813
8	1.7236	Sucrose	Up	Down	387.1144
9	2.3647	Imidazole lactic acid	Up	Up	157.0607
10	1.6524	Alpha-ketoisovaleric acid	–	Up	115.0391
11	1.7116	Phenylpyruvic acid	–	Up	163.0393
12	2.7184	Indole-3-acetaldehyde	–	Up	158.0604
13	2.5721	Ferulic acid	–	Up	193.0501
14	2.2609	Isopropylmaleic acid	–	Up	157.0499
15	2.2763	Sinapoyl aldehyde	Down	–	207.0657
16	2.5483	Phenylacetic acid	–	Up	135.0443
17	3.2287	N-hydroxyl-tryptamine	–	Down	221.0928
18	2.4611	Phenyllactic acid	–	Up	165.0550
19	2.8042	Dulcitol	Down	Down	181.0711
20	1.5032	D-arabitol	Up	Up	151.0604
21	1.8555	P-anisic acid	–	Up	151.0393
22	2.0281	Galactinol	Up	Down	377.0854
23	2.1379	Myo-inositol	Down	Down	215.0323
24	2.2035	L-aspartate-semialdehyde	–	Up	116.0344
25	1.9992	Digalacturonic acid	–	Up	351.0567
26	1.8172	Trans-aconitic acid	Up	–	173.0085
27	2.8109	4-methylbenzyl alcohol	–	Down	267.1337
28	2.4326	Pretyrosine	–	Down	269.1131
29	2.4152	Gamma-glutamyl-L-putrescine	–	Down	218.1498
30	1.7101	N-carbamoylputrescine	–	Up	173.1396
31	1.7799	5-acetamidovalerate	–	Down	360.2129
32	1.7322	3-indoleacetic acid	Up	Up	174.0554
33	2.2463	6-hydroxyhexanoic acid	–	Up	131.0705
34	2.8826	S-adenosyl-L-homocysteine	–	Down	383.1140
35	1.9836	Glucosamine	–	Up	160.0608
36	1.7660	Mesaconic acid	–	Up	129.0184
37	1.9886	Phenylacetylglutamine	Up	Down	309.1092
38	2.4756	Trehalose	Up	–	360.1495

(Continues)

TABLE 2 (Continued)

	VIP	Metabolite	SCZ	SZZ	M/Z
39	1.5107	L-proline	Up	–	116.0708
41	2.5029	D-mannose 6-phosphate	Up	–	259.0222
42	1.9570	5-hydroxyindoleacetic acid	Down	–	190.0503
43	2.6574	Hydantoin-5-propionic acid	Down	–	171.0405
44	2.3487	D-ribulose 5-phosphate	Up	–	211.0007
45	1.5975	L-methionine	Down	–	148.0429
46	2.7195	N-acetyl-l-glutamicacetyl-l-glutamic acid	Up	–	188.0558
47	1.8743	5-hydroxy-L-tryptophan	Down	–	219.0770
48	1.5649	Oxoglutaric acid	Down	–	191.0191
49	1.6329	Glycolaldehyde	Down	–	179.0555
50	1.5081	Adipic acid	Down	–	145.0498
51	1.5368	3-hydroxyphenylacetic acid	Down	–	151.0393
52	2.3536	Coniferaldehyde	Down	–	223.0608
53	1.6988	Vanillin	Down	–	151.0393
54	1.6098	N2-acetyl-L-ornithine	Down	–	173.0924
55	1.6006	L-phenylalanine	Down	–	164.0710
56	3.4732	Pantothenic acid	Up	–	218.1030
57	1.5624	Pyrocatechol	Down	–	109.0286
58	1.7690	Homogentisic acid	Down	–	167.0343
59	1.7557	Aspartic acid	Up	–	132.0294
60	1.8214	Uridine diphosphate-N-acetylglucosamine	Down	–	606.0742
61	2.0683	3-methyl-2-oxovaleric acid	Up	–	131.0703
62	2.2592	N6-(L-1,3-dicarboxypropyl)-L-lysine	Up	–	275.1247
63	1.7804	L-histidine	Up	Down	156.0767
64	1.8998	Tryptophol	–	Up	162.0913
65	−1.7731	5-methoxyindoleacetate	Up	–	247.1075

Abbreviations: SCZ, stone cell group; SNZ, supernatant group; -, representatives in the corresponding group did not detect the corresponding differential metabolites.

Studies have shown that the combined action of these three enzymes is more effective in degrading cellulose (Fernandes et al., 2022; Krisztina et al., 2022). Our findings showed that three *L. plantarum* strains used in the project had low cellulose degradation potential which appears to be further reduced over fermentation time. This was possibly related to the weak enzyme production capacity of the strains in single culture. Bacterial interaction in mixed cultures have been reported to enhance the cellulose degradation potential of the community (Detain et al., 2022; Karuppiah et al., 2022). Therefore, in this study cellulose degradation was carried out in single as well as mixed cultures (bacteria with yeast) to see how bacterial interactions may affect this process. A significant increase in the enzyme activity of the mixed cultures was observed probably due to metabolic or some unknown interactions between *L. plantarum* and the yeast. It was reported that *L. plantarum* in single culture fermentation lowers the pH of the medium which negatively affects the cellulase activity or stability, whereas the addition of *S. cerevisiae* helps to keep the pH at the optimum level required for the maximum cellulase activity and production by utilizing the metabolites produced by lactic acid bacteria

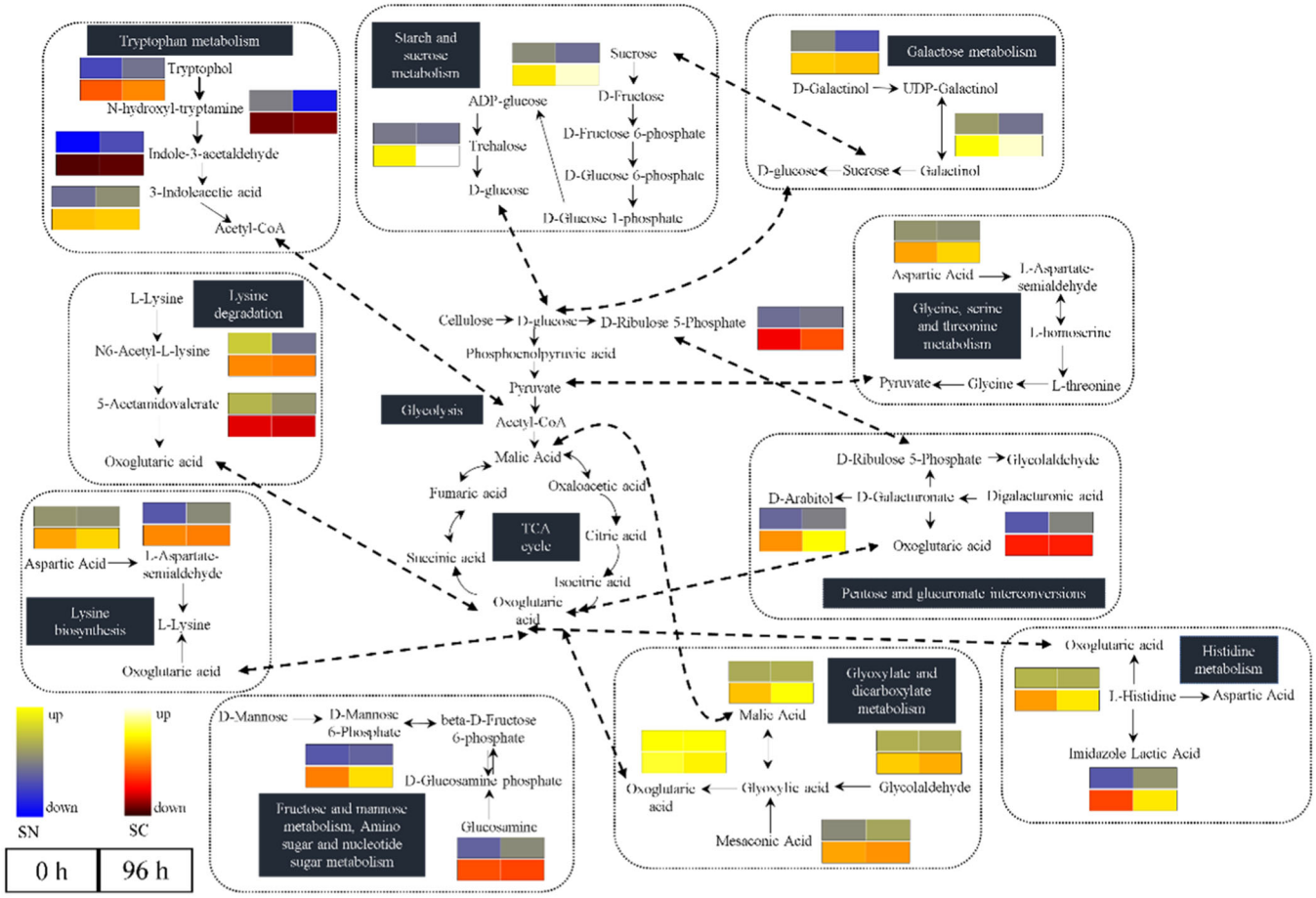

FIGURE 6 The key carbohydrate metabolism and amino acid metabolism involved in differential metabolites in stone cell degradation. The bar chart from blue to yellow annotated as SN in the figure represents the change of metabolite abundance in the supernatant group. The bar chart from black to white annotated as SC represents the change of metabolite abundance in the stone cell group. The box on the left represents the metabolite abundance at 0 h of fermentation, and the box on the right represents 96 h of fermentation.

(Hirai & Kawasumi, 2020; Huang, Feng, et al., 2021; Saroj et al., 2022). *S. cerevisiae* also produces cellulase (Zhang et al., 2019), which enhances the overall volume of the enzyme. In line with the above-mentioned results, cellulose content of the stone cells subjected to the mixed culture fermentation were lowest compared to other stone cells which underwent fermentation with single strains. To further explore the degradation of stone cells, we used SEM to observe the morphology of different stone cell samples. The results showed that the surface of the fer-mented stone cells became rough and porous, possibly due to microbial hydrolysis leading to degradation of the stone cells with changes in the dense structure (Danso et al., 2022), and the degradation effect was more pronounced in case of mixed-culture fermentation.

The FTIR gives qualitative and semi-quantitative information regarding functional groups in stone cells (Huang, Yu, et al., 2021). Therefore, FTIR was used to determine the changes in the chemical structure of the cell surface of stone cells belonging to different groups (Supporting Information S1: Table 1). The characteristic peaks of the stone cells cultured with the mixed culture containing *L. plantarum* JYLP-326 and *S. cerevisiae* Y2 for 96 h decreased compared with those cultured with the single strain of *L. plantarum* (JYLP-326) for at 0 and 96 h. The absorption peak at 3348 cm^{-1} represents the association between hydroxyl groups in stone cells. Therefore, the intensity of the absorption peak at 3348 cm^{-1} is weakened and widened, indicating that the association between hydroxyl groups in stone cells is weakened. which is conducive to the depolymerization of cellulose and hemicellulose (Wei et al., 2022). The absorption peak near 2924 cm^{-1} represents the stretching vibration of cellulose (C-H), and the intensity of absorption peak of stone cells co-fermented by *L. plantarum* JYLP-326 and *S. cerevisiae* Y2 weakened here, which indicates that the cellulose structure in the stone cells that underwent mixed culture fermentation became disordered (Dar et al., 2022; Ren et al., 2021). The absorption peak intensity of stone cells following mixed fermentation decreased at 1430 cm^{-1}, indicating that the crystal structure of cellulose I could be degraded by mixed fermentation (Wei et al., 2022).

The intensity of the absorption peak at 1258 cm^{-1} of the stone cells that underwent mixed fermentation was lower than that of the stone cells that underwent single culture fermentation. which also indicates the fracture of C-H bond in hemicellulose. The absorption peak at 1031 cm^{-1} is due to the tensile vibration peak of C-O-H of sugar ring in cellulose and C-O in C-O-C. After mixed-culture with *L. plantarum* JYLP-326 and *S. cerevisiae* Y2, the peak of stone cells at this point was weakened, indicating that the C-O bond in cellulose is broken and cellulose is degraded (Lin et al., 2020). In addition, the intensity of peaks at 1735 and 1515 cm^{-1} in the mixed-culture fermentation samples were lower than those in the other two groups, which represented the degradation of functional groups related to the extension of lignin structure. These results indicated some degradation of lignin (Usman et al., 2022), which is generally attached to the surface of cellulose and thus it hinders degradation of cellulose (Lu et al., 2022). The other peak at 1735 cm^{-1} represents the extension of the ester bond of the acetyl group in hemicellulose. A decrease in the intensity of the absorption peak at this point is an indication of the damage caused to ester bond and degradation of hemicellulose (Lin et al., 2020). Altogether mixed fermentation turned out to be an effective approach in degrading cellulose, lignin, and hemicellulose in stone cells.

The presence of characteristic peaks in the crystal plane (110 and 004) of cellulose I by the X-ray diffraction pattern of stone cells indicates the presence of amorphous regions, and similar results have been observed in the characterization of cellulose in cassava peels and dragon peels (Taharuddin et al., 2023). In addition, a reduction in cellulose crystallinity is a clear indication of the disruption of cellulose structure (Ma et al., 2020), which is linked to the degradation of stone cells. According to the results of this study, the crystallinity of the fermented stone cells was effectively reduced, which is possibly linked to the degradation of cellulose and hemicellulose in the stone cells by the enzymes of *L. plantarum* and *S. cerevisiae* (Si et al., 2022). In addition, a decrease of crystallinity of lignocellulose as a result of the degradation of cellulose and hemicellulose has been observed in many previous studies (Zhang et al., 2022; Zhang, Shah, et al., 2021). The results of XRD and FTIR also confirmed that cellulose in stone cells was effectively degraded after fermentation.

A previous study used metagenomics to confirm the metabolic functional potential of microbial consortia that could grow and degrade corn stover and filter paper. It was found that synergistic interactions among the bacterial strains led to enhanced lignocellulolytic potential of the communities which showed upregulation of carbohydrate metabolic and amino acid metabolic pathways (Borjigin et al., 2022).

By summarizing the results of previous studies, it can be concluded that microorganisms interact synergistically to degrade cellulose into cellobiose using endoglucanase and exoglucanase, and the cellobiose further cleaved through hydrolysis pathway and phosphorylation pathway. The hydrolysis pathway requires the use of β-glucosidase to break down cellobiose into small molecules of glucose, which are then further metabolized by glycolysis (Li et al., 2019).

The cellulose in the stone cells was degraded into glucose by hydrolysis in the cell, and the glucose was subjected to glycolysis and the TCA cycle to produce malic acid. Therefore, the content of malic acid in stone cells increased on 96 h fermentation. Zhang also found that the main metabolites involved in the TCA cycle stimulate cellulose degradation by bacteria belonging to the phylum Bacteroidetes (Zheng et al., 2021). In addition, malic acid can also be produced by glycolaldehyde and mesaconic acid because α-ketoglutarate is a precursor for the synthesis of lysine, and α-ketoglutarate is not only consumed in the TCA cycle, but it is also consumed by the synthesis of lysine, which is also the reason why the content of oxoglutaric acid does not change significantly(Fan et al., 2022). Glucose was not detected in either the stone cell group or the supernatant group, probably because glucose was converted to pyruvate and then entered the TCA cycle, which also provided more energy for microbial growth. In addition, the results show that the amino acid metabolic pathway is also an essential part of the microbial degradation of cellulose (Figure 6). Among them, aspartic acid, L-histidine, and tryptophan are precursors for the production of oxoglutaric acid and acetyl-CoA (Li, Wang, et al., 2022). The increase in the abundance of these substances can promote the TCA cycle and produce more energy. Studies have shown that starch-sucrose metabolism was also among important metabolic pathways in the process of cellulose degradation (Dong et al., 2022). Sucrose and trehalose in the stone cell group and the supernatant group were annotated to this pathway, and the abundance of these two substances was observed in the stone cell group, but the inverse was observed for the supernatant group, which could be due to continuous production of sucrose and trehalose by microbial degradation of stone cells. Sucrose and trehalose in the supernatant can be used as carbon sources by lactic acid bacteria and yeast (Sieuwerts et al., 2018).

Hemicellulose is a heterogeneous polymer composed of several different types of monosaccharides. The glycosyl groups that constitute hemicellulose mainly include D-xylose, D-mannose, D-glucose, D-galactose, L-arabinose, 4-O-methyl-D-glucuronic acid, D-galacturonic acid and D-glucuronic acid (Wang et al., 2019). The contents of 4-O-alpha-D-galactopyranuronosyl-D-galacturonic acid, 6-phosphate D-mannose, D-arabitol, and D-ribulose 5-phosphate in differential metabolites increased, which indicates hemicellulose degradation to produce corresponding monosaccharides and further metabolism. The decrease in D-galactose content is due to its metabolism into

galactinol and D-glucose. In addition, pyrocatechol, vanillin, phenylacetic acid, ferulic acid were detected in differential metabolites. The presence of the above-mentioned metabolites indicates lignin degradation (Li & Zheng, 2020; Niu et al., 2021; Zhu et al., 2023). Therefore, the mixed-culture of lactic acid bacteria and yeast resulted in the degradation of lignin in stone cells. In summary, the results show that the mixed-culture fermentation involving lactic acid bacteria and yeasts can effectively degrade cellulose, hemicellulose and lignin in stone cells which can help to get rid of stone cells in pears.

5 | CONCLUSION

In this study, a dual-species culture comprising *L. plantarum* JYLP-326 and *S. cerevisiae* Y2 has been reported as an optimum fermentation culture to degrade stone cells in pears. When stone cells originated from pears were subjected to mixed-culture fermentation, a degradation rate of 37.67% was observed after 96 h of fermentation where 82.26% reduction in cellulose content was recorded. Our findings were further confirmed by structural and topographical changes in stone cells following different types of fermentation. The absorption peaks associated with lignin (1515, 1378 cm^{-1}), cellulose (1031, 1430, 1378, 2902 cm^{-1}) and hemicellulose (3335, 1378 cm^{-1}) changed significantly in the mixed-culture fermentation system and the crystallinity of the stone cells decreased. The relative abundance of metabolites such as malic acid, α-ketoglutaric acid, galactose, D-arabinitol, vanillin, and ferulic acid in the stone cells medium changed as a result of the mixed-culture fermentation, and these changes indicate degradation of stone cells through carbohydrate metabolism, amino acid metabolism and other related pathways.

AUTHOR CONTRIBUTIONS

Jie Gao: Writing—original draft; conceptualization; methodology; software; writing—review & editing; funding acquisition. **Chao Xu**: Conceptualization; data curation; formal analysis; methodology; writing—original draft. **Guifang Tian**: Data curation; software. **YueHong Ji**: Supervision; writing—review and editing. **Faizan Ahmed Sadiq**: Conceptualization; writing—review & editing. **Ke Wang**: Supervision; writing—review and editing. **Yaxin Sang**: Supervision; writing—review & editing; funding acquisition; resources; project administration. All authors have read and agreed to the published version of the manuscript.

ACKNOWLEDGMENTS

Thanks to Hebei Agricultural University for the help of the experiment. This research was supported by Hebei Modern Agricultural Industrial Technology System (HBCT2024170206).

CONFLICT OF INTEREST STATEMENT

The authors declare no conflicts of interest.

DATA AVAILABILITY STATEMENT

Data sets generated and/or analyzed in the current study can be obtained from corresponding authors upon reasonable request.

ETHICS STATEMENT

None declared.

ORCID

Jie Gao http://orcid.org/0000-0002-8334-1569

REFERENCES

Ajeje, S. B., Hu, Y., Song, G., Peter, S. B., Afful, R. G., Sun, F., Asadollahi, M. A., Amiri, H., Abdulkhani, A., & Sun, H. (2021). Thermostable cellulases/xylanases from thermophilic and hyperthermophilic microorganisms: Current perspective. *Frontiers in Bioengineering and Biotechnology*, *9*(2021), 794304. https://doi.org/10.3389/fbioe.2021.794304

Al Talebi, Z. A., Al-Kawaz, H. S., Mahdi, R. K., Al-Hassnawi, A. T., Alta'ee, A. H., Hadwan, A. M., khudhair, D. A., & Hadwan, M. H. (2022). An optimized protocol for estimating cellulase activity in biological samples. *Analytical Biochemistry*, *655*, 114860. https://doi.org/10.1016/j.ab.2022.114860

An, X., Zong, Z., Zhang, Q., Li, Z., Zhong, M., Long, H., Cai, C., & Tan, X. (2022). Novel thermo-alkali-stable cellulase-producing Serratia sp. AXJ-M cooperates with Arthrobacter sp. AXJ-M1 to improve degradation of cellulose in papermaking black liquor. *Journal of Hazardous Materials*, *421*, 126811. https://doi.org/10.1016/j.jhazmat.2021.126811

Balla, A., Silini, A., Cherif-Silini, H., Bouket, A. C., Boudechicha, A., Luptakova, L., Alenezi, F. N., & Belbahri, L. (2022). Screening of cellulolytic bacteria from various ecosystems and their cellulases production under multi-stress conditions. *Catalysts*, *12*(7), 769. https://doi.org/10.3390/catal12070769

Borjigin, Q., Zhang, B., Yu, X., Gao, J., Zhang, X., Qu, J., Ma, D., Hu, S., & Han, S. (2022). Metagenomics study to compare the taxonomic composition and metabolism of a lignocellulolytic microbial consortium cultured in different carbon conditions. *World Journal of Microbiology & Biotechnology*, *38*(5), 78. https://doi.org/10.1007/s11274-022-03260-1

Cai, T., Xi, P. S., Kou, C. C., Zhang, Y. Y., Cao, X. H., & Zhu, D. S. (2021). Study on juice yield by compound enzymolysis in cloudy apple juice. *Materials Science Forum*, *1032*(2021), 45–50. https://doi.org/10.4028/WWW.SCIENTIFIC.NET/MSF.1032.45

Chen, K.-J., Tang, J.-C., Xu, B.-H., Lan, S.-L., & Cao, Y. (2019). Degradation enhancement of rice straw by co-culture of *Phanerochaete chrysosporium* and *Trichoderma viride*. *Scientific Reports*, *9*, 19708. https://doi.org/10.1038/s41598-019-56123-5

Chen, Z., Wang, Y., Cheng, H., & Zhou, H. (2022). Hemicellulose degradation: An overlooked issue in acidic deep eutectic solvents pretreatment of lignocellulosic biomass. *Industrial Crops and Products*, *187*(PA), 115335. https://doi.org/10.1016/j.indcrop.2022.115335

Danso, B., Ali, S. S., Xie, R., & Sun, J. (2022). Valorisation of wheat straw and bioethanol production by a novel xylanase-and cellulase-producing *Streptomyces* strain isolated from the wood-feeding termite, *Microcerotermes* species. *Fuel*, *310*, 122333. https://doi.org/10.1016/j.fuel.2021.122333

Dar, M. A., Syed, R., Pawar, K. D., Dhole, N. P., Xie, R., Pandit, R. S., & Sun, J. (2022). Evaluation and characterization of the cellulolytic bacterium, *Bacillus pumilus* SL8 isolated from the gut of oriental leafworm *Spodoptera litura*: An assessment of

its potential value for lignocellulose bioconversion. *Environmental Technology & Innovation*, *27*, 102459. https://doi.org/10.1016/j.eti.2022.102459

Detain, J., Rémond, C., Rodrigues, C. M., Harakat, D., & Besaury, L. (2022). Co-elicitation of lignocelluloytic enzymatic activities and metabolites production in an *Aspergillus-Streptomyces* co-culture during lignocellulose fractionation. *Current Research in Microbial Sciences*, *3*, 100108. https://doi.org/10.1016/j.crmicr.2022.100108

Dobrzyński, J., Wróbel, B., & Górska, E. B. (2022). Cellulolytic properties of a potentially lignocellulose-degrading bacillus sp. 8E1A strain isolated from bulk soil. *Agronomy*, *12*(3), 665. https://doi.org/10.3390/agronomy12030665

Dong, M., Wang, S., Xu, F., Xiao, G., Bai, J., Wang, J., & Sun, X. (2022). Integrative transcriptome and proteome analyses of *Trichoderma longibrachiatum* LC and its cellulase hyper-producing mutants generated by heavy ion mutagenesis reveal the key genes involved in cellulolytic enzymes regulation. *Biotechnology for Biofuels and Bioproducts*, *15*(1), 63. https://doi.org/10.1186/s13068-022-02161-7

Fan, W., Huang, X., Liu, K., Xu, Y., Hu, B., & Chi, Z. (2022). Nutrition component adjustment of distilled dried grain with solubles via aspergillus Niger and its change about dynamic physiological metabolism. *Fermentation*, *8*(6), 264. https://doi.org/10.3390/fermentation8060264

FAO. (2021). *Production quantities of Pears by country*. http://www.fao.org/faostat/home/statistics/FAOSTAT-data-production-cropsandlivestockproducts-pears

Fernandes, C. G., Sawant, S. C., Mule, T. A., Khadye, V. S., Lali, A. M., & Odaneth, A. A. (2022). Enhancing cellulases through synergistic β-glucosidases for intensifying cellulose hydrolysis. *Process Biochemistry*, *120*(2022), 202–212. https://doi.org/10.1016/J.PROCBIO.2022.06.011

Hanan Taharuddin, N., Jumaidin, R., Ridzuan Mansor, M., Asyadi Md Yusof, F., & Hanim Alamjuri, R. (2023). Characterization of potential cellulose from *Hylocereus polyrhizus* (Dragon Fruit) peel: A study on physicochemical and thermal properties. *Journal of Renewable Materials*, *11*(1), 131–145. https://doi.org/10.32604/jrm.2022.021528

Hirai, S., & Kawasumi, T. (2020). Enhanced lactic acid bacteria viability with yeast coincubation under acidic conditions. *Bioscience, Biotechnology, and Biochemistry*, *84*(8), 1706–1713. https://doi.org/10.1080/09168451.2020.1756213

Huang, C., Feng, Y., Patel, G., Xu, X., Qian, J., Liu, Q., & Kai, G. (2021). Production, immobilization and characterization of beta-glucosidase for application in cellulose degradation from a novel *Aspergillus versicolor*. *International Journal of Biological Macromolecules*, *177*, 437–446. https://doi.org/10.1016/j.ijbiomac.2021.02.154

Huang, Y., Yu, Q., Li, M., Jin, S., Fan, J., Zhao, L., & Yao, Z. (2021). Surface modification of activated carbon fiber by low-temperature oxygen plasma: Textural property, surface chemistry, and the effect of water vapor adsorption. *Chemical Engineering Journal*, *418*(7532), 129474. https://doi.org/10.1016/j.cej.2021.129474

Karuppiah, V., Zhixiang, L., Liu, H., Murugappan, V., Kumaran, S., Perianaika Anahas, A. M., & Chen, J. (2022). Co-cultivation of T. asperellum GDFS1009 and B. amyloliquefaciens 1841: Strategy to regulate the production of ligno-cellulolytic enzymes for the lignocellulose biomass degradation. *Journal of Environmental Management*, *301*, 113833. https://doi.org/10.1016/j.jenvman.2021.113833

Kim, K. H., Dutta, T., Sun, J., Simmons, B., & Singh, S. (2018). Biomass pretreatment using deep eutectic solvents from lignin derived phenols. *Green Chemistry*, *20*(4), 809–815. https://doi.org/10.1039/c7gc03029k

Kurnia Ila, R., & Astuti Feb, F. (2021). Screening of cellulolytic bacteria from biological education and Research Forest Floor Andalas University, Indonesia. *Pakistan Journal of Biological Sciences*, *24*(5), 612–617. https://doi.org/10.3923/pjbs.2021.612.617

Langan, P., Cnanakaran, S., Rector, K. D., Pawley, N. m, Fox, D. T., Cho, D. W., & Hammel, K. E. (2011). Exploring new strategies for cellulosic biofuels production. *Energy & Environmental Science: EES*, *4*(10), 3820–3833. https://doi.org/10.1039/C1EE01268A

Li, F., Xie, Y., Gao, X., Shan, M., Sun, C., Niu, Y. D., & Shan, A. (2020). Screening of cellulose degradation bacteria from Min pigs and optimization of its cellulase production. *Electronic Journal of Biotechnology*, *48*, 29–35. https://doi.org/10.1016/j.ejbt.2020.09.001

Li, J., Gu, S., Zhao, Z., Chen, B., Liu, Q., Sun, T., Sun, W., & Tian, C. (2019). Dissecting cellobiose metabolic pathway and its application in biorefinery through consolidated bioprocessing in *Myceliophthora thermophila*. *Fungal Biology and Biotechnology*, *6*, 21. https://doi.org/10.1186/s40694-019-0083-8

Li, J., Wang, S., Zhao, J., Dong, Z., & Shao, T. (2022). Gut microbiota of *Ostrinia nubilalis* larvae degrade maize cellulose. *Frontiers in Microbiology*, *13*, 816954. https://doi.org/10.3389/fmicb.2022.816954

Li, X., Han, C., Li, W., Chen, G., & Wang, L. (2020). Insights into the cellulose degradation mechanism of the thermophilic *Funguschaetomium* thermophilumbased on integrated functional omics. *Biotechnology for Biofuels*, *13*(1), 143. https://doi.org/10.1186/s13068-020-01783-z

Li, X., & Zheng, Y. (2020). Biotransformation of lignin: Mechanisms, applications and future work. *Biotechnology Progress*, *36*(1), e2922. https://doi.org/10.1002/btpr.2922

Li, Y., Zhang, P., Zhu, D., Yao, B., Hasunuma, T., Kondo, A., & Zhao, X. (2022). Efficient preparation of soluble inducer for cellulase production and saccharification of corn stover using in-house generated crude enzymes. *Biochemical Engineering Journal*, *178*(2022), 108296. https://doi.org/10.1016/j.bej.2021.108296

Lin, D., Long, X., Huang, Y., Yang, Y., Wu, Z., Chen, H., Zhang, Q., Wu, D., Qin, W., & Tu, Z. (2020). Effects of microbial fermentation and microwave treatment on the composition, structural characteristics, and functional properties of modified okara dietary fiber. *LWT*, *123*, 109059. https://doi.org/10.1016/j.lwt.2020.109059

Lin, S., Lin, D., Wu, B., Ma, S., Sun, S., Zhang, T., Zhang, W., Bai, Y., Wang, Q., & Wu, J. (2022). Morphological and developmental features of stone cells in eriobotrya fruits. *Frontiers in Plant Science*, *13*(2022), 823993. https://doi.org/10.3389/fpls.2022.823993

Liu, X., Qi, Y., Lian, J., Song, J., Zhang, S., Zhang, G., Fan, J., & Zhang, N. (2022). Construction of actinomycetes complex flora in degrading corn straw and an evaluation of their degradative effects. *Biotechnology Letters*, *44*(12), 1477–1493. https://doi.org/10.1007/s10529-022-03313-3

Lu, H., Liu, S., Shi, Y., & Chen, Q. (2022). Efficient delignification of sugarcane bagasse by Fenton oxidation coupled with ultrasound-assisted NaOH for biotransformation from *Agaricus sinodeliciosus* var. Chaidam. *Chemical Engineering Journal*, *448*(2022), 137719. https://doi.org/10.1016/j.cej.2022.137719

Ma, L., Lu, Y., Yan, H., Wang, X., Yi, Y., Shan, Y., Liu, B., Zhou, Y., & Lü, X. (2020). Screening of cellulolytic bacteria from rotten wood of Qinling (China) for biomass degradation and cloning of cellulases from *Bacillus methylotrophicus*. *BMC Biotechnology*, *20*(1), 2. https://doi.org/10.1186/s12896-019-0593-8

Ma, Q., Ji, Q., Chen, L., Zhu, Z., Tu, S., Okonkwo, C. E., Out, P., & Zhou, C. (2022). Multimode ultrasound and ternary deep eutectic solvent sequential pretreatments enhanced the enzymatic saccharification of corncob biomass. *Industrial Crops and Products*, *188*, 115574. https://doi.org/10.1016/j.indcrop.2022.115574

Mamat, A., Tusong, K., Xu, J., Yan, P., Mei, C., & Wang, J. (2021). Integrated transcriptomic and proteomic analysis reveals the complex molecular mechanisms underlying stone cell formation in Korla pear. *Scientific Reports*, *11*(1), 7688. https://doi.org/10.1038/s41598-021-87262-3

Niu, J., Li, X., Qi, X., & Ren, Y. (2021). Pathway analysis of the biodegradation of lignin by *Brevibacillus thermoruber*. *Bioresource Technology*, *341*(8), 125875. https://doi.org/10.1016/j.biortech.2021.125875

Pasha, I., Ahmad, F., & Usman, M. (2021). Elucidation of morphological characteristics, crystallinity, and molecular structures of native and enzyme modified cereal brans. *Journal of Food Biochemistry*, *45*(7), e13768. https://doi.org/10.1111/jfbc.13768

Pérez-Alvarado, O., Zepeda-Hernández, A., Garcia-Amezquita, L. E., Requena, T., Vinderola, G., & García-Cayuela, T. (2022). Role of lactic acid bacteria and yeasts in sourdough fermentation during breadmaking: Evaluation of postbiotic-like components and health benefits. *Frontiers in Microbiology*, *13*, 969460. https://doi.org/10.3389/fmicb.2022.969460

Qinggeer, Gao, J., Yu, X., Zhang, B., Wang, Z., Naoganchaolu, B., Hu, S., Sun, J., Xie, M., & Wang, Z. (2016). Screening of a microbial consortium with efficient corn stover degradation ability at low temperature. *Journal of Integrative Agriculture*, *15*(10), 2369–2379. https://doi.org/10.1016/s2095-3119(15)61272-2

Ren, H., Sun, W., Yan, Z., Zhang, Y., Wang, Z., Song, B., Zheng, Y., & Li, J. (2021). Bioaugmentation of sweet sorghum ensiling with rumen fluid: Fermentation characteristics, chemical composition, microbial community, and enzymatic digestibility of silages. *Journal of Cleaner Production*, *294*, 126308. https://doi.org/10.1016/j.jclepro.2021.126308

Ren, Z., You, W., Wu, S., Poetsch, A., & Xu, C. (2019). Secretomic analyses of *Ruminiclostridium papyrosolvens* reveal its enzymatic basis for lignocellulose degradation. *Biotechnology for Biofuels*, *12*(1), 183. https://doi.org/10.1186/s13068-019-1522-8

Renye, J. A. Jr., White, A. K., & Hotchkiss, A. T. Jr. (2021). Identification of *Lactobacillus* strains capable of fermenting Fructo-Oligosaccharides and inulin. *Microorganisms*, *9*(10), 2020. https://doi.org/10.3390/microorganisms9102020

Saroj, P., P, M., & Narasimhulu, K. (2022). Biochemical characterization of thermostable carboxymethyl cellulase and β-glucosidase from *Aspergillus fumigatus* JCM 10253. *Applied Biochemistry and Biotechnology*, *194*(2022), 2503–2527. https://doi.org/10.1007/s12010-022-03839-2

Sheladiya, P., Kapadia, C., Prajapati, V., Ali El Enshasy, H., Abd Malek, R., Marraiki, N., Zaghloul, N. S. S., & Sayyed, R. Z. (2022). Production, statistical optimization, and functional characterization of alkali stable pectate lyase of *Paenibacillus lactis* PKC5 for use in juice clarification. *Scientific Reports*, *12*(1), 7564. https://doi.org/10.1038/s41598-022-11022-0

Shi, Z., Han, C., Zhang, X., Tian, L., & Wang, L. (2020). Novel synergistic mechanism for lignocellulose degradation by a thermophilic filamentous fungus and a thermophilic actinobacterium based on functional proteomics. *Frontiers in Microbiology*, *11*(020), 539438. https://doi.org/10.3389/fmicb.2020.539438

Si, J., Yang, C., Ma, W., Chen, Y., Xie, J., Qin, X., Hu, X., & Yu, Q. (2022). Screen of high efficiency cellulose degrading strains and effects on tea residues dietary fiber modification: Structural properties and adsorption capacities. *International Journal of Biological Macromolecules*, *220*, 337–347. https://doi.org/10.1016/j.ijbiomac.2022.08.092

Sieuwerts, S., Bron, P. A., & Smid, E. J. (2018). Mutually stimulating interactions between lactic acid bacteria and *Saccharomyces cerevisiae* in sourdough fermentation. *LWT*, *90*, 201–206. https://doi.org/10.1016/j.lwt.2017.12.02

Su, Y., Yu, X., Sun, Y., Wang, G., Chen, H., & Chen, G. (2018). Evaluation of screened lignin-degrading fungi for the biological pretreatment of corn stover. *Scientific Reports*, *8*(1), 5385. https://doi.org/10.1038/s41598-018-23626-6

Tatsumi, D., Kanda, A., & Kondo, T. (2022). Characterization of mercerized cellulose nanofibrils prepared by aqueous counter collision process. *Journal of Wood Science*, *68*(1), 13. https://doi.org/10.1186/s10086-022-02019-4

Tulsani, N. J., Jakhesara, S. J., Hinsu, A. T., Jyotsana, B., Dafale, N. A., Patil, N. V., Purohit, H. J., & Joshi, C. G. (2022). Genome analysis and CAZy repertoire of a novel fungus *Aspergillus sydowii* C6d with lignocellulolytic ability isolated from camel rumen. *Electronic Journal of Biotechnology*, *59*, 36–45. https://doi.org/10.1016/j.ejbt.2022.06.0040717-3458

Usman, S., Li, F., An, D., Shou, N., Deng, J., Zhang, Y., Guo, X., & Shen, Y. (2022). Lignocellulose degradation and enzymatic hydrolysis of soybean incorporated sorghum silage inoculated with feruloyl-esterase producing *Lactobacillus plantarum*. *Fermentation*, *8*(2):70. https://doi.org/10.3390/fermentation8020070

Viesser, J. A., de Melo Pereira, G. V., de Carvalho Neto, D. P., Rogez, H., Góes-Neto, A., Azevedo, V., Brenig, B., Aburjaile, F., & Soccol, C. R. (2021). Co-culturing fructophilic lactic acid bacteria and yeast enhanced sugar metabolism and aroma formation during cocoa beans fermentation. *International Journal of Food Microbiology*, *339*, 109015. https://doi.org/10.1016/j.ijfoodmicro.2020.109015

Wang, C., Yang, J., Wen, J., Bian, J., Li, M., Peng, F., & Sun, R. (2019). Structure and distribution changes of *Eucalyptus* hemicelluloses during hydrothermal and alkaline pretreatments. *International Journal of Biological Macromolecules*, *133*, 514–521. https://doi.org/10.1016/j.ijbiomac.2019.04.127

Wang, L., Zhang, H., & Lei, H. (2022). Phenolics profile, antioxidant activity and flavor volatiles of pear juice: Influence of lactic acid fermentation using three *Lactobacillus* strains in monoculture and binary mixture. *Foods*, *11*(1), 11. https://doi.org/10.3390/foods11010011

Wang, X., Wang, P., Su, Y., Wang, Q., Ling, Z., & Yong, Q. (2022). Supramolecular deconstruction of bamboo holocellulose via hydrothermal treatment for highly efficient enzymatic conversion at low enzyme dosage. *International Journal of Molecular Sciences*, *23*(19), 11829. https://doi.org/10.3390/ijms231911829

Wei, J., Gao, H., Li, Y., & Nie, Y. (2022). Research on the degradation behaviors of wood pulp cellulose in ionic liquids. *Journal of Molecular Liquids*, *356*, 119071. https://doi.org/10.1016/j.molliq.2022.119071

Wu, X., Amanze, C., Wang, J., Yu, Z., Shen, L., Wu, X., Li, J., Yu, R., Liu, Y., & Zeng, W. (2022). Isolation and characterization of a novel thermotolerant alkali lignin-degrading bacterium *Aneurinibacillus* sp. LD3 and its application in food waste composting. *Chemosphere*, *307*(Pt3), 135859. https://doi.org/10.1016/j.chemosphere.2022.135859

Xue, C., Yao, J.-L., Qin, M.-F., Zhang, M.-Y., Allan, A. C., Wang, D.-F., & Wu, J. (2018). PbrmiR397a regulates lignification during stone cell development in pear fruit. *Plant Biotechnology Journal*, *17*(1), 103–117. https://doi.org/10.1111/pbi.12950

Yan, C., Zhang, N., Xu, C., Jin, Q., Qi, Y., & Cai, Y. (2023). Effects on stone cell development and lignin deposition in pears by different pollinators. *Frontiers in Plant Science*, *14*, 1093661. https://doi.org/10.3389/fpls.2023.1093661

Yang, M., Zhao, J., Yuan, Y., Chen, X., Yang, F., & Li, X. (2021). Comparative metagenomic discovery of the dynamic cellulose-degrading process from a synergistic cellulolytic microbiota. *Cellulose*, *28*(4), 2105–2123. https://doi.org/10.1007/s10570-020-03671-z

Yang, X., Zhao, F., Yang, L., Li, J., & Zhu, X. (2022). Enhancement of the aroma in low-alcohol apple-blended pear wine mixed fermented with *Saccharomyces cerevisiae* and non-saccharomyces yeasts. *LWT*, *155*, 112994. https://doi.org/10.1016/j.lwt.2021.112994

Zajki-Zechmeister, K., Eibinger, M., & Nidetzky, B. (2022). Enzyme synergy in transient clusters of endo- and exocellulase enables a multilayer mode of processive depolymerization of cellulose. *ACS Catalysis*, *12*(17), 10984–10994. https://doi.org/10.1021/ACSCATAL.2C02377

Zhang, B., Wendan, Y., Wang, F., Omedi, J. O., Liu, R., Huang, J., Zhang, L., Zou, Q., Huang, W., & Li, S. (2019). Use of *Kluyveromyces marxianus* prefermented wheat bran as a source of enzyme mixture to improve dough performance and bread

biochemical properties. *Cereal Chemistry*, *96*(1), 142–153. https://doi.org/10.1002/cche.10125

Zhang, C., & Wang, F. (2020). Catalytic lignin depolymerization to aromatic chemicals. *Accounts of Chemical Research*, *53*(2), 470–484. https://doi.org/10.4028/WWW.SCIENTIFIC.NET/MSF.1032.45

Zhang, H., Li, Z., Zhang, H., Li, Y., Wang, F., Xie, H., Su, L., & Song, A. (2022). Biodegradation of gramineous lignocellulose by *Locusta migratoria manilensis* (Orthoptera: Acridoidea). *Frontiers in Bioengineering and Biotechnology*, *10*, 943692. https://doi.org/10.3389/fbioe.2022.943692

Zhang, Y., Dai, Z., Zhou, Z., Yin, H., Zhang, M., Zhang, H., Liu, Y., Li, Q., Nan, X., Liu, X., & Meng, D. (2021). Development of the yeast and lactic acid bacteria co-culture agent for atmospheric ammonia removing: Genomic features and on-site applications. *Ecotoxicology and Environmental Safety*, *218*(6), 112287. https://doi.org/10.1016/j.ecoenv.2021.112287

Zhang, Z., Shah, A. M., Mohamed, H., Tsiklauri, N., & Song, Y. (2021). Isolation and screening of microorganisms for the effective pretreatment of lignocellulosic agricultural wastes. *BioMed Research International*, *2021*, 5514745. https://doi.org/10.1155/2021/5514745

Zhao, S. S., Wang, Y. P., Yang, F. Y., Wang, Y., & Zhang, H. (2020). Screening a *Lactobacillus plantarum* strain for good adaption in alfalfa ensiling and demonstrating its improvement of alfalfa silage quality. *Journal of Applied Microbiology*, *129*(2), 233–242. https://doi.org/10.1111/jam.14604

Zheng, P., Zhang, M., Fang, X., Tang, L., Wang, Z., & Shi, F. (2022). Analysis of the fruit quality of pear (Pyrus spp.) using widely targeted metabolomics. *Foods*, *11*(10), 1440. https://doi.org/10.3390/foods11101440

Zheng, R., Cai, R., Liu, R., Liu, G., & Sun, C. (2021). Maribellus comscasis sp. nov., a novel deep-sea *Bacteroidetes* bacterium, possessing a prominent capability of degrading cellulose. *Environmental Microbiology*, *23*(8), 4561–4575. https://doi.org/10.1111/1462-2920.15650

Zhou, B., Ma, C., Ren, X., Xia, T., & Li, X. (2020). LC-MS/MS-based metabolomic analysis of caffeine-degrading fungus *Aspergillus sydowii* during tea fermentation. *Journal of Food Science*, *85*(2), 477–485. https://doi.org/10.1111/1750-3841.15015

Zhu, N., Zhu, Y., Li, B., Jin, H., & Dong, Y. (2021). Increased enzyme activities and fungal degraders by *Gloeophyllum trabeum* inoculation improve lignocellulose degradation efficiency during manure-straw composting. *Bioresource Technology*, *337*(337), 125427. https://doi.org/10.1016/j.biortech.2021.125427

Zhu, X., Zhou, Z., Guo, G., Li, J., Yan, H., & Li, F. (2023). Proteomics and metabolomics analysis of the lignin degradation mechanism of lignin-degrading fungus *Aspergillus fumigatus* G-13. *Analytical Methods*, *15*(8), 1062–1076. https://doi.org/10.1039/d2ay01446g

SUPPORTING INFORMATION

Additional supporting information can be found online in the Supporting Information section at the end of this article.

How to cite this article: Gao, J., Xu, C., Tian, G., Ji, Y. H., Sadiq, F. A., Wang, K., & Sang, Y. (2024). A study revealing mechanisms behind the stone cell of Yali pear degradation by mixed-culture fermentation of lactic acid bacteria and yeast. *eFood*, *5*(3), e153. https://doi.org/10.1002/efd2.153